

Provided for non-commercial research and education use.  
Not for reproduction, distribution or commercial use.



This article was published in an Elsevier journal. The attached copy is furnished to the author for non-commercial research and education use, including for instruction at the author's institution, sharing with colleagues and providing to institution administration.

Other uses, including reproduction and distribution, or selling or licensing copies, or posting to personal, institutional or third party websites are prohibited.

In most cases authors are permitted to post their version of the article (e.g. in Word or Tex form) to their personal website or institutional repository. Authors requiring further information regarding Elsevier's archiving and manuscript policies are encouraged to visit:

<http://www.elsevier.com/copyright>



# Rheological modelling of residual stresses and deformations of plates during non-uniform cooling

Giovanni Buratti, Maurizio Froli\*

*Dipartimento di Ingegneria Strutturale dell' Università di Pisa, Italy*

Received 7 September 2006; received in revised form 26 March 2007; accepted 15 April 2007

Available online 4 May 2007

---

## Abstract

The time–space distribution of eigen-stresses and residual deformations of a plane plate which reaches its final solid state through a given transition process of non-uniform cooling is described here by means of a simple visco-elastic rheological model.

The aging processes of the elastic and viscous properties are supposed to be temperature dependant in order to directly control the influence of the thermal history on the final stress and deformation conditions of the solid.

The model is able to reproduce qualitatively well the development of eigen-stresses in the spatially symmetrical cooling processes of tempering or toughening, as well as the formation of eigen-stresses and permanent bending in the spatially asymmetrical cooling processes of heat curving.

© 2007 Elsevier Ltd. All rights reserved.

*Keywords:* Rheological model; Transient eigen-stresses; Visco-elasticity; Relaxation; Tempering; Heat curving

---

## 1. Introduction

At early stages of the manufacturing process, a great part of structural materials and components find themselves in a state of very high temperature and very low solid consistence. Through the subsequent transient phase of progressive cooling down, the material or the component gradually achieves its final solid state as for example in steel plates after the rolling treatment or in glass panes during heat tempering. A similar process develops also in a young concrete wall where the inner production of hydration heat and the insulating action of the forms cause initially a quasi uniform temperature distribution that turns to a transient cooling process when the forms are removed and the lateral surfaces directly interact with the cooler open air (see for example Ref. [1]).

In all the cases, if the rate of heat exchange at the outer surfaces is relatively high in comparison to the thermal conductivity of the material—i.e. the Biot number is large—a transient non-isothermal cooling down phase

takes place through the thickness of the plate and before thermal equilibrium is finally reached, temperature changes non-linearly with respect to time and space.

Coupled with the thermodynamical aspects of the problem, mechanical effects take also place in form of transient distributions of eigen-stresses and deformations.

It is well known that non-linear temperature distributions cause in a solid self-equilibrated thermal stresses (primary eigen-stresses) whatever the mechanical properties of the material are and even if the body is completely free from outer restrains, but if during the transient period of cooling any part of the material has not yet crossed the transformation temperature, corresponding to a significant increase in Young's modulus and viscosity, non-linear thermal deformations are compensated by the flow of the still soft material and eigen-stresses quickly vanish.

However, from the instant at which the temperature of the outer surfaces has reached this transformation value, the stiffening front propagates from the borders inwards. At this time the inner warmer layers of the body continue to contract following the cooling progression but this contraction is restrained by the colder, already stiff outer layers giving rise, when the stiffening process has

---

\*Corresponding author.

E-mail address: [m.froli@ing.unipi.it](mailto:m.froli@ing.unipi.it) (M. Froli).

completed, to a complex system of non-stationary eigen-stresses—generally compressive at the surfaces and tensile in the interior—which would remain permanently locked in the material if relaxation phenomena would not take place. Additionally, in a cooling process that progresses symmetrically with respect to the mean plane of the plate, residual deformations are at each time step also symmetrical; consequently the plate remains at every instant plane and at the end of the process a mean general contraction of its initial dimensions is the only evident irreversible deformation. Such properties are at the basis of heat treatments like toughening of steel plates and hardening or tempering of float glass panes.

If the cooling process develops not symmetrically with respect of the mean plane, the plate curves at any time under the combined effect of thermal volume changes, elastic and creep strains. Once again, due to the non-uniform and not simultaneous stiffening process over the thickness and even when the final stage of uniform temperature is reached, a residual permanent curvature takes place in addition to the general uniform contraction and also, of course, to thermal eigen-stresses. This effect, called heat curving, is widely used to fabricate structural steel girders for curved bridges. Following this procedure, steel beams are submitted to multiple heat/cool cycles, each of them resulting in a cumulative permanent deformation [2] that partially vanishes with time under the effects of relaxation.

Due to the increasing demand coming from many different industrial fields for a sound theory able to model temperature dependent stiffening processes of structural components and to predict their final stress and deformation state, generations of mechanicians have worked at the development of a general non-linear theory of thermo-visco-elasticity which could give solutions to all this class of problems.

Numberless books and contributions have been devoted to such a complex theme where mechanical effects are strongly coupled with thermodynamics (see for example, Refs. [3,4]). Very frequently entire special research currents and ramifications have formed within this field, each one devoted to a particular material (see for example the contributions gathered in Ref. [5]). In the impossibility to cite all the relevant contributions, we have chosen to recall here two works of Müller [6,7] for what metals are concerned, and two of Bažant for what concrete is concerned [8,9].

In most cases, however, following a purely phenomenological approach, uncoupled linear viscoelasticity has been used to predict eigen-stresses in solidification processes produced by heat loss.

Therefore, thermal stresses in concrete at early ages have been calculated in a simplified way by Nagy [10] while concrete aging has been described in integral form by Carol and Bažant [9] which have schematized a elementary portion of the material by means of Maxwell and Kelvin chains whose components progressively solidify. All the

moduli are assumed to vary proportionally to a single time dependant aging function taken as the ratio between the solidified volume at a generic instant and the final volume of the body. The authors assumed also that the new layers of material being solidified join the constituent ones in a parallel coupling.

Studying glass solidification, Lee et al. [11], for example, tried to describe mathematically stress and structural relaxation in the field of thermal annealing or tempering of this material by means of a visco-elastic model, extended later by Gardon and Narayanaswamy [12–15], based on the experimental observations of Kurkijan that glass behaves as a thermodynamically simple visco-elastic material [16]. Soules et al. [17] and more recently Laufs [18], have implemented the Narayanaswamy visco-elastic model in FEM library programs in order to accurately predict the development of tempering stresses from the knowledge of the thermal history of the glass plate and the temperature dependence of its visco-elastic properties.

In this study we have also adopted a phenomenological approach schematizing a plane plate by means of a very simple discrete rheological model composed by a parallel assemblage of Maxwell chains submitted to prescribed thermal histories and whose visco-elastic properties are given as regular functions of temperature.

Aim of the paper is just to indicate an engineering-like, practical procedure for analytically predicting time and space distributions of eigen-stresses and permanent deformations in plane plates during temperature dependent stiffening processes.

## 2. Basic assumptions

Let us consider the simple case of a large rectangular plate which is initially at a uniform, relatively high temperature. The plate is at the beginning of a stiffening process which progresses, within a certain transition period, from the outer to the inner surfaces as a consequence of its cooling down to a final lower, uniformly distributed thermal field next to the room temperature.

During the transient period the heat losses are supposed to be uniformly distributed at each instant all over the two external surfaces. At sufficient distance from the edges the instantaneous temperature distribution varies just over the plate thickness; the whole problem has therefore a cylindrical symmetry with respect of any  $y$ -axis normal to the plate (Fig. 1).

We suppose moreover that the time–space distributions of the thermal fields are completely known during the transient period.

The solidification process is here simulated by attributing to the material known, visco-elastic temperature dependant properties, based on experimental data, such that elasticity approaches asymptotically its final value within the transition period while viscosity tends, in the same interval, to disappear.

The aim is to predict the time progression of the distributions of residual stresses through the thickness during the transient phase of solidification.

### 3. Statement of the problem

Let us subdivide the plate into a finite number of thin sheets parallel to the mean plane. Due to the polar symmetry of the problem, at a sufficient distance from the borders the deformation state at any point  $O$  of each sheet is completely described by the radial strain along a generic direction  $r$  from  $O$  parallel to the sheet. The mechanical behaviour of a single strip may therefore be schematized by a Maxwell chain succession of three units: an elastic spring, a viscous dashpot, a thermal unit,

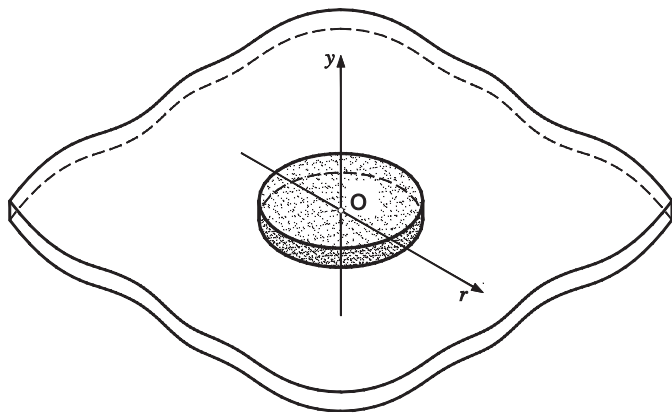


Fig. 1. Cylindrical symmetry of the problem.

provided that  $y_i$  indicates the distance of the  $i$ th sheet from the mean plane (Fig. 2).

The thermal element is submitted to the prescribed thermal history of the related strip, while the mechanical properties of the elastic and the viscous unit follow a given temperature dependance.

We assume also that the classic Kirchhoff hypothesis applies, i.e. the strain distribution along the plate thickness is linear at sufficient distance from the edges.

The complete calculation scheme thus consists in a Kelvin chain arrangement of such strip-elements, as shown schematically in Fig. 3.

Let the number of elements into which the plate is subdivided be  $2n$ , each element being identified by its index  $i$  ( $i = 1, 2, \dots, 2n$ ).

Let us denote with  $\varepsilon_i^e$ ,  $\dot{\varepsilon}_i^v$  and  $\varepsilon_i^T$ , respectively, the strain in the elastic spring, in the dashpot and in the thermal unit. If  $\sigma_i^e$  is the stress and  $E_i$  the elastic modulus of the spring,  $\sigma_i^v$  is the stress,  $\lambda_i$  the viscous coefficient of the dashpot and  $\alpha_i$  is the coefficient of thermal expansion, then we can write

$$\varepsilon_i^e = \frac{\sigma_i^e}{E_i}, \tag{3.1a}$$

$$\dot{\varepsilon}_i^v = \frac{\sigma_i^v}{\lambda_i}, \tag{3.1b}$$

$$\varepsilon_i^T = \alpha_i \Delta T_i, \tag{3.1c}$$

where the dot indicates the time derivation and  $\Delta T_i$  is the variation of temperature in the  $i$ th element.

Expressions (3.1), may be used with sufficient accuracy also in the case when the material is submitted to a large

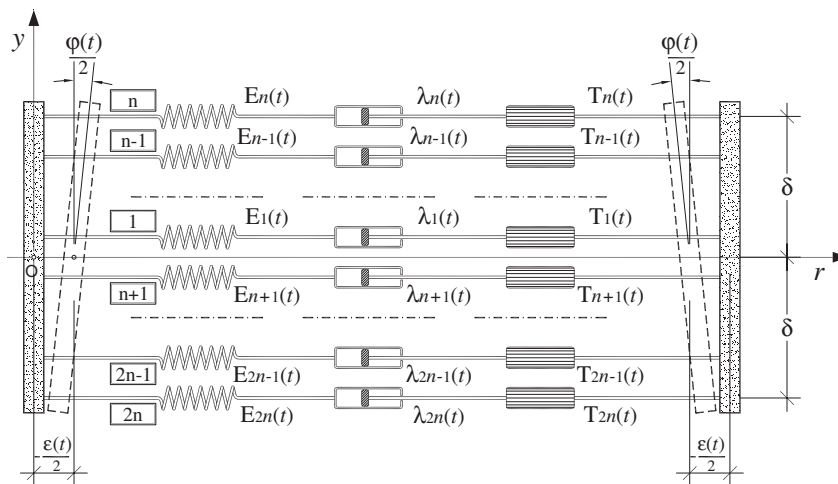


Fig. 2. Calculation scheme.

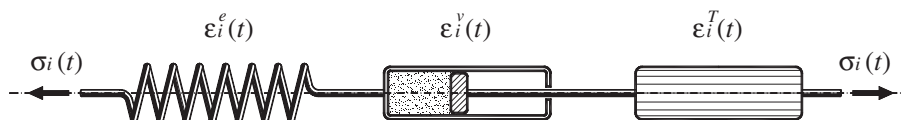


Fig. 3. The rheological model for the  $i$ th element.

variation of temperature; in this case it is sufficient to consider  $E$ ,  $\lambda$  and  $\alpha$  appropriate and known functions of  $T : E(T); \lambda(T); \alpha(T)$ .

Since the three elements—*spring*, *dashpot* and *thermal cell*—are connected in series, the total strain of each strip can be written as

$$\varepsilon_i = \varepsilon_i^e + \varepsilon_i^v + \varepsilon_i^T, \quad (3.2)$$

while the stress acting on the chain of three elements must be the same

$$\sigma_i^e = \sigma_i^v = \sigma_i^T = \sigma_i. \quad (3.3)$$

If the body undergoes non-uniform change of temperature, the strains due to the thermal expansion or contraction will be consequently non-uniform. Since each strip is not free to expand longitudinally, being bounded to neighbouring strips by the hypothesis of strain linearity over the thickness, the application of these strains will give rise to stresses in the longitudinal direction and, in turn, to viscous deformations.

Let us consider the system shown in Fig. 2. The body is supposed to have initially a uniform temperature  $T_0$ . Later, during the cooling process, the temperature profile is no more uniform within the thickness and changes with time.

The distribution of eigen-stresses evolves as well but, since it starts from a self-equilibrated state, it must maintain self-equilibrium at every instant.

In order to evaluate the stress distribution through the thickness of the plate, we assume that the elastic, viscous and thermal components of the strain are regular functions of time and differentiate with respect to time the compatibility equations (3.2).

Taking into account Eqs. (3.1a) and (3.3) we get

$$\frac{d\varepsilon_i}{dt} = \frac{d\sigma_i}{dt E_i} + \frac{\sigma_i}{\lambda_i} + \frac{d}{dt}(\alpha\Delta T)_i. \quad (3.4)$$

Assuming

$$\sigma_i(0) = \bar{\sigma}_i = 0, \quad (3.5)$$

the problem is to find a set of  $2n$  functions  $\sigma_i(t)$  and  $2n$  functions  $\varepsilon_i(t)$  that satisfy Eq. (3.4) and the conditions that the body is stress-free in the initial state. In order to reduce (3.4) to a more convenient form, let us consider the instantaneous equilibrium equations

$$\sum_{i=1}^{2n} \sigma_i = 0 \quad (3.6a)$$

and

$$\sum_{i=1}^{2n} \sigma_i y_i = 0. \quad (3.6b)$$

Their derivatives with respect to time yield the following:

$$\frac{d}{dt} \sum_{i=1}^{2n} \sigma_i = 0 \quad (3.7a)$$

and

$$\frac{d}{dt} \sum_{i=1}^{2n} \sigma_i y_i = 0, \quad (3.7b)$$

that can be rewritten as

$$\sum_{i=1}^{2n} \frac{d\sigma_i}{dt} = 0 \quad (3.8a)$$

and

$$\sum_{i=1}^{2n} \frac{d\sigma_i}{dt} y_i = 0, \quad (3.8b)$$

considering also  $\sigma_i$  regular functions of time and hypothesizing  $y_i$  not time depending.

Since

$$\sigma_i = \sigma_i^e = E_i \varepsilon_i^e, \quad (3.9)$$

(3.8a) and (3.8b) can be thus expressed as functions of the elastic strain:

$$\sum_{i=1}^{2n} \frac{d}{dt} (E_i \varepsilon_i^e) = \sum_{i=1}^{2n} E_i \frac{d\varepsilon_i^e}{dt} + \sum_{i=1}^{2n} \frac{dE_i}{dt} \varepsilon_i^e = 0, \quad (3.10a)$$

$$\sum_{i=1}^{2n} \frac{d}{dt} (E_i \varepsilon_i^e) y_i = \sum_{i=1}^{2n} E_i \frac{d\varepsilon_i^e}{dt} y_i + \sum_{i=1}^{2n} \frac{dE_i}{dt} \varepsilon_i^e y_i = 0. \quad (3.10b)$$

But we know, from (3.2), that  $\varepsilon_i^e = \varepsilon_i - \varepsilon_i^v - \varepsilon_i^T$ , then we obtain

$$\sum_{i=1}^{2n} E_i \frac{d(\varepsilon_i - \varepsilon_i^v - \varepsilon_i^T)}{dt} + \sum_{i=1}^{2n} \frac{dE_i}{dt} \varepsilon_i^e = 0 \quad (3.11a)$$

and

$$\sum_{i=1}^{2n} E_i \frac{d(\varepsilon_i - \varepsilon_i^v - \varepsilon_i^T)}{dt} y_i + \sum_{i=1}^{2n} \frac{dE_i}{dt} \varepsilon_i^e y_i = 0. \quad (3.11b)$$

Now we observe that, according to Kirchhoff's hypothesis, the total strain of each strip can be expressed by the following linear relation:

$$\varepsilon_i = \varepsilon(t) - \varphi(t) y_i \quad (i = 1, \dots, 2n), \quad (3.12)$$

where  $\varepsilon(t)$  and  $\varphi(t)$  are, respectively, the average strain and the relative rotation between the ends of the mechanical model (see Fig. 2). Thus, the  $2n$  unknown functions  $\varepsilon_i(t)$  can be replaced by the only two  $\varepsilon(t)$  and  $\varphi(t)$ . Eqs. (3.11a) and (3.11b) become thus, respectively,

$$\sum_{i=1}^{2n} E_i \frac{d[(\varepsilon - \varphi y_i) - \varepsilon_i^v - \varepsilon_i^T]}{dt} + \sum_{i=1}^{2n} \frac{\sigma_i}{E_i} \frac{dE_i}{dt} = 0 \quad (3.13a)$$

and

$$\sum_{i=1}^{2n} E_i \frac{d[(\varepsilon - \varphi y_i) - \varepsilon_i^v - \varepsilon_i^T]}{dt} y_i + \sum_{i=1}^{2n} \frac{\sigma_i}{E_i} \frac{dE_i}{dt} y_i = 0. \quad (3.13b)$$

Since  $\varepsilon$  and  $\varphi$  are not involved in the sum, we can write

$$\frac{d\varepsilon}{dt} \sum_{i=1}^{2n} E_i - \frac{d\varphi}{dt} \sum_{i=1}^{2n} E_i y_i - \sum_{i=1}^{2n} E_i \frac{d\varepsilon_i^v}{dt} - \sum_{i=1}^{2n} E_i \frac{d\varepsilon_i^T}{dt} + \sum_{i=1}^{2n} \frac{dE_i}{dt} \varepsilon_i^e = 0 \quad (3.14a)$$

and

$$\frac{d\varepsilon}{dt} \sum_{i=1}^{2n} E_i y_i - \frac{d\varphi}{dt} \sum_{i=1}^{2n} E_i y_i^2 - \sum_{i=1}^{2n} E_i \frac{d\varepsilon_i^v}{dt} y_i - \sum_{i=1}^{2n} E_i \frac{d\varepsilon_i^T}{dt} y_i + \sum_{i=1}^{2n} \frac{dE_i}{dt} \varepsilon_i^e y_i = 0. \quad (3.14b)$$

The two previous equations form a linear algebraic system from which the unknown time derivatives of  $\varepsilon$  and  $\varphi$  can then be readily obtained. The result is

$$\dot{\varepsilon} = \frac{\sum E_i y_i^2 \sum [E_i \dot{\varepsilon}_i^v + E_i \dot{\varepsilon}_i^T - (\sigma_i/E_i) \dot{E}_i] - \sum E_i y_i \sum [E_i \dot{\varepsilon}_i^v y_i + E_i \dot{\varepsilon}_i^T y_i - (\sigma_i/E_i) \dot{E}_i y_i]}{\sum E_i \sum E_i y_i^2 - (\sum E_i y_i)^2}, \quad (3.15)$$

and

$$\dot{\varphi} = \frac{\sum E_i y_i \sum [E_i \dot{\varepsilon}_i^v + E_i \dot{\varepsilon}_i^T - (\sigma_i/E_i) \dot{E}_i] - \sum E_i \sum [E_i \dot{\varepsilon}_i^v y_i + E_i \dot{\varepsilon}_i^T y_i - (\sigma_i/E_i) \dot{E}_i y_i]}{\sum E_i \sum E_i y_i^2 - (\sum E_i y_i)^2}, \quad (3.16)$$

where the summatory extremes are understood being extended from  $i = 1$  to  $2n$ .

Now, let us consider the terms included into brackets. By adopting the expressions for the strains given by (3.1b) and (3.1c), we get after some calculations

$$E_i \dot{\varepsilon}_i^v + E_i \dot{\varepsilon}_i^T - \frac{\sigma_i}{E_i} \dot{E}_i = E_i \sigma_i \left( \frac{1}{\lambda_i} + \frac{d}{dt} \frac{1}{E_i} \right) + E_i \frac{d(\alpha \Delta T)_i}{dt} \quad (3.17)$$

and

$$E_i \dot{\varepsilon}_i^v y_i + E_i \dot{\varepsilon}_i^T y_i - \frac{\sigma_i}{E_i} \dot{E}_i y_i = E_i \sigma_i \left( \frac{1}{\lambda_i} + \frac{d}{dt} \frac{1}{E_i} \right) y_i + E_i \frac{d(\alpha \Delta T)_i}{dt} y_i, \quad (3.18)$$

so that, with the position

$$\frac{1}{\Phi_i} = \frac{1}{\lambda_i} + \frac{d}{dt} \frac{1}{E_i}, \quad (3.19)$$

expressions (3.15) and (3.16) assume, respectively, the form

$$\dot{\varepsilon} = \frac{\sum E_i y_i^2 \sum [(E_i/\Phi_i) \sigma_i + E_i d(\alpha \Delta T)_i/dt] - \sum E_i y_i \sum [(E_i/\Phi_i) \sigma_i y_i + E_i (d(\alpha \Delta T)_i/dt) y_i]}{\sum E_i \sum E_i y_i^2 - (\sum E_i y_i)^2} \quad (3.20)$$

and

$$\dot{\varphi} = \frac{\sum E_i y_i \sum [(E_i/\Phi_i) \sigma_i + E_i d(\alpha \Delta T)_i/dt] - \sum E_i \sum (E_i/\Phi_i) \sigma_i y_i + E_i (d(\alpha \Delta T)_i/dt) y_i]}{\sum E_i \sum E_i y_i^2 - (\sum E_i y_i)^2} \quad (3.21)$$

We see that the time derivatives of  $\varepsilon$  and of  $\varphi$  can be calculated provided we know the evolution of the stress functions  $\sigma_i$ , of  $E_i$ ,  $\lambda_i$  and of  $(\alpha_i \Delta T_i)$  during time. Consequently, the derivative of the strain in each strip, unknown in (3.4), can be expressed in terms of the same variables since, from (3.12),

$$\frac{d\varepsilon_i}{dt} = \frac{d\varepsilon(t)}{dt} - \frac{d\varphi(t)}{dt} y_i \quad (i = 1, \dots, 2n). \quad (3.22)$$

Thus, with the help of Eqs. (3.20) and (3.21), that express the instantaneous equilibrium of the body, we can finally rewrite the set of ordinary differential equations (3.4) whose solution gives, together with the initial conditions (3.5), the researched  $2n$  functions  $\sigma_i(t)$ . The set assumes the following form:

$$\frac{d\sigma_i}{dt} + \frac{E_i}{\Phi_i} \sigma_i + E_i \frac{d(\alpha \Delta T)_i}{dt} + K_i \left\{ \left( y_i \sum E_j y_j - \sum E_j y_j^2 \right) \times \sum \left[ \frac{E_j}{\Phi_j} \sigma_j + E_j \frac{d(\alpha \Delta T)_j}{dt} \right] - \left( y_i \sum E_j - \sum E_j y_j \right) \times \sum \left[ \frac{E_j}{\Phi_j} \sigma_j y_j + E_j \frac{d(\alpha \Delta T)_j}{dt} y_j \right] \right\} = 0, \quad (3.23)$$

where we introduced the further notation

$$K_i = \frac{E_i}{\sum E_j \sum E_j y_j^2 - (\sum E_j y_j)^2}. \quad (3.24)$$

Once obtained the stress functions  $\sigma_i(t)$ , the components of strain due to elastic and viscous effects are, respectively, given by (3.1a) and (3.1b).

#### 4. Applications

In order to demonstrate the capability of the model to qualitatively well reproduce time and space distributions of

eigen-stresses for different prescribed cooling histories, the following numerical examples are given. In all the applications the plate, of thickness  $2\delta$ , has been subdivided with a set of 20 units.

4.1. Symmetrical cooling

Due to the symmetry of the problem the plate remains plane, thus

$$\varphi = 0, \tag{4.1a}$$

$$\dot{\varphi} = 0 \tag{4.1b}$$

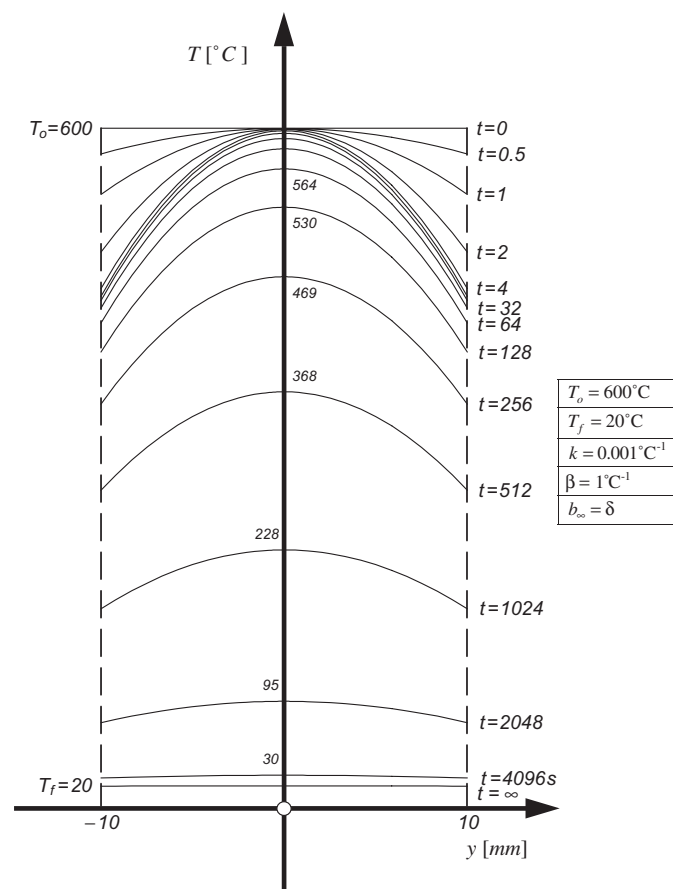


Fig. 4. Tempering thermal history (1st case).

and

$$\dot{\epsilon} = \frac{\sum E_i y_i^2 \sum [(E_i/\Phi_i)\sigma_i + E_i d(\alpha\Delta T)/dt]}{\sum E_i \sum E_i y_i^2} \tag{4.2}$$

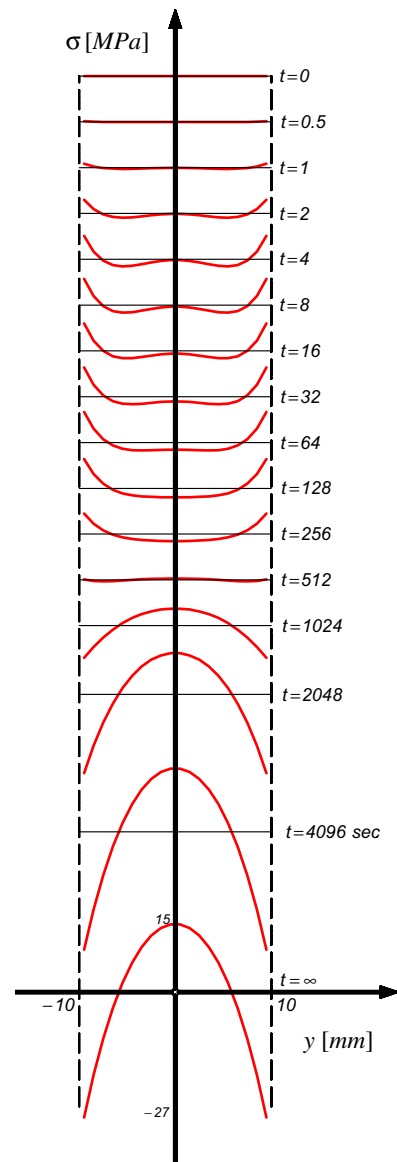


Fig. 6. Tempering eigen-stresses generation (1st case).

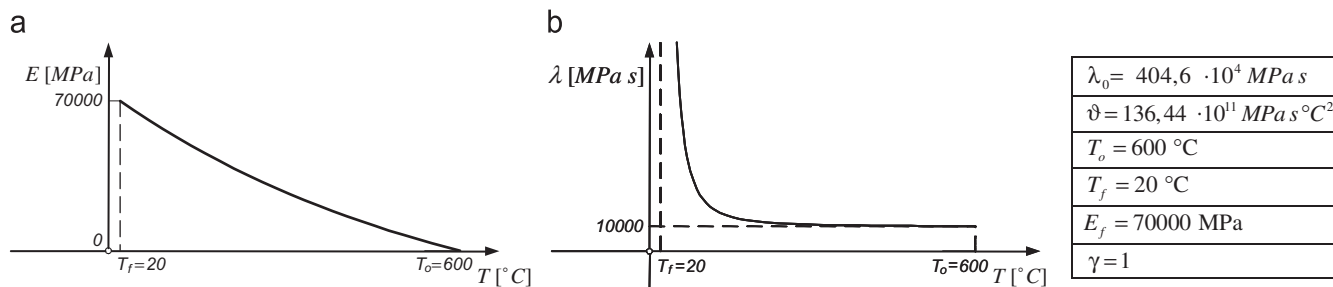


Fig. 5. (a) Elastic modulus versus temperature. (b) Viscous coefficient versus temperature.

The set of differential equations reduces of course into

$$\frac{d\sigma_i}{dt} + \frac{E_i}{\Phi_i} \sigma_i + E_i \frac{d(\alpha \Delta T)_i}{dt} + K_i \left\{ - \sum E_j y_j^2 \sum \left[ \frac{E_j}{\Phi_j} \sigma_j + E_j \frac{d(\alpha \Delta T)_j}{dt} \right] \right\} = 0. \quad (4.3)$$

In the following, three examples are presented to illustrate the time evolution of eigen-stresses in a plate as consequence of symmetrical cooling.

4.1.1. Heat tempering: first case

A very large glass pane, initially at the uniform temperature of  $T_0 = 600^\circ\text{C}$ , undergoes a given, arbitrary cooling process described by

$$T(y, t) = T_f + (T_0 - T_f) e^{-kt} \left\{ 1 - \left[ \frac{y}{b_\infty} (1 - e^{-\beta t}) \right]^2 \right\}, \quad (4.4)$$

and illustrated in Fig. 4, whose shape well approximate temperature fields during tempering treatments [19]. Fig. 4 collects also the set of thermal parameters assumed in the present example.

It can be seen that in the first 4 s the temperature of the outer surfaces diminishes of about  $130^\circ\text{C}$  but from that

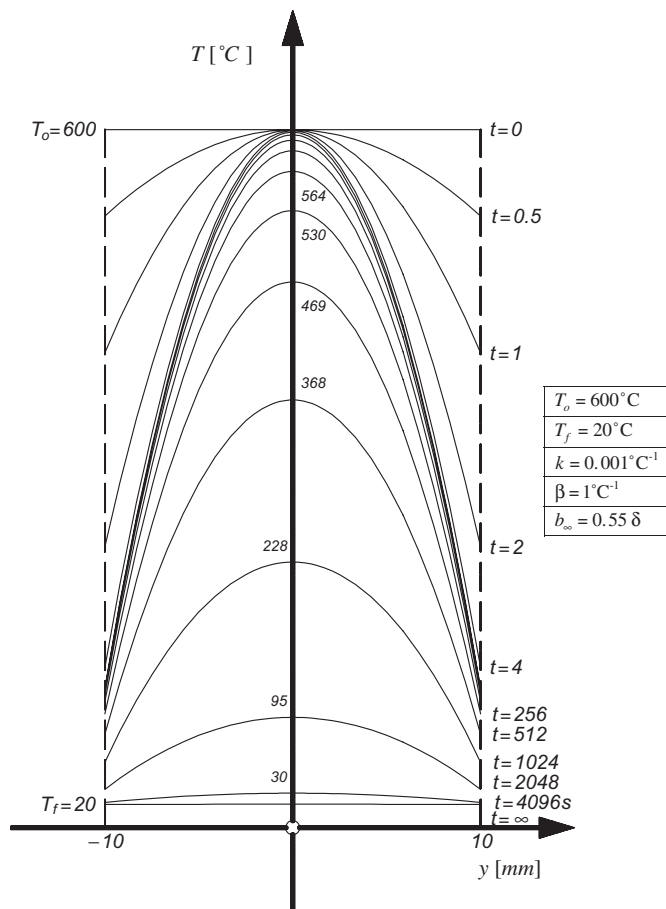


Fig. 7. Tempering thermal history (2nd case).

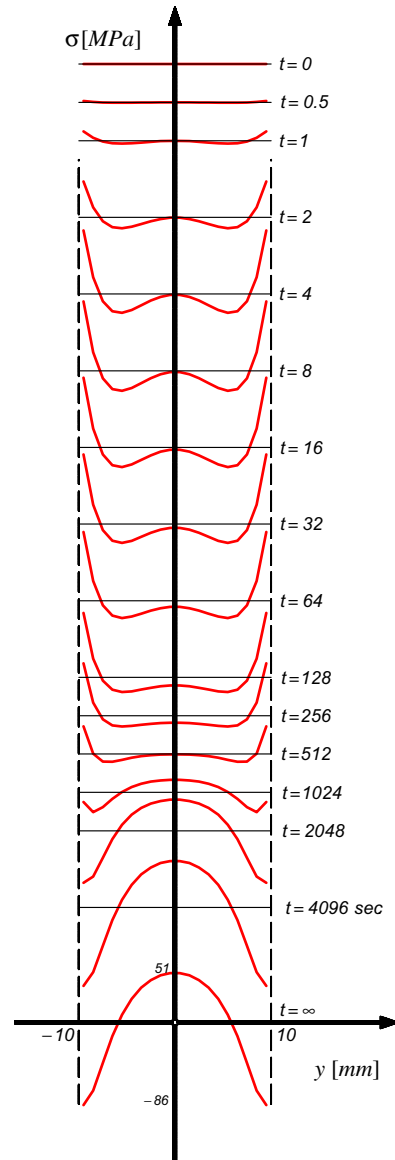


Fig. 8. Tempering eigen-stresses generation (2nd case).

instant on the cooling proceeds rather slowly with reduced thermal gradients within the thickness  $2\delta$  and is completed after circa 2000 s.

We assume moreover that the elastic modulus of the material and the viscosity coefficient depend on temperature, respectively, following Eqs. (4.5a) and (4.5b) so that, at a room temperature of  $T_f = 20^\circ\text{C}$ , elasticity has reached its final value and practically there is not any further viscous deformation (see Figs. 5a and b):

$$E(T) = E_f \frac{1 - e^{\gamma(T_0 - T)/(T_0 - T_f)}}{1 - e^\gamma}, \quad (4.5a)$$

$$\lambda(T) = -\lambda_0 + \frac{\vartheta}{(T - T_f)^2}. \quad (4.5b)$$

The solution of the set of differential equations (3.23), numerically performed with the help of programme MATHEMATICA [20], allows to calculate the generation of the

tempering eigen-stresses through the thickness of the plate at the different instants of the transition phase (see Fig. 6).

The form of the instantaneous distributions well resembles available experimental data (see for example, Ref. [6]) and it can be noticed that surface eigen-stresses, which are tensile before  $t = 1024$ s, turn after that instant to compression and begin to grow up to the final level of about 27MPa while tensile eigen-stresses migrate towards the middle part of the plate and reach a final intensity of 15MPa.

4.1.2. Heat tempering: second case

Let us consider again the same hypothetical thermal history, described by Eq. (4.4) with a different set of parameters, as indicated in Fig. 7 which collects also some isothermal curves of this cooling down process.

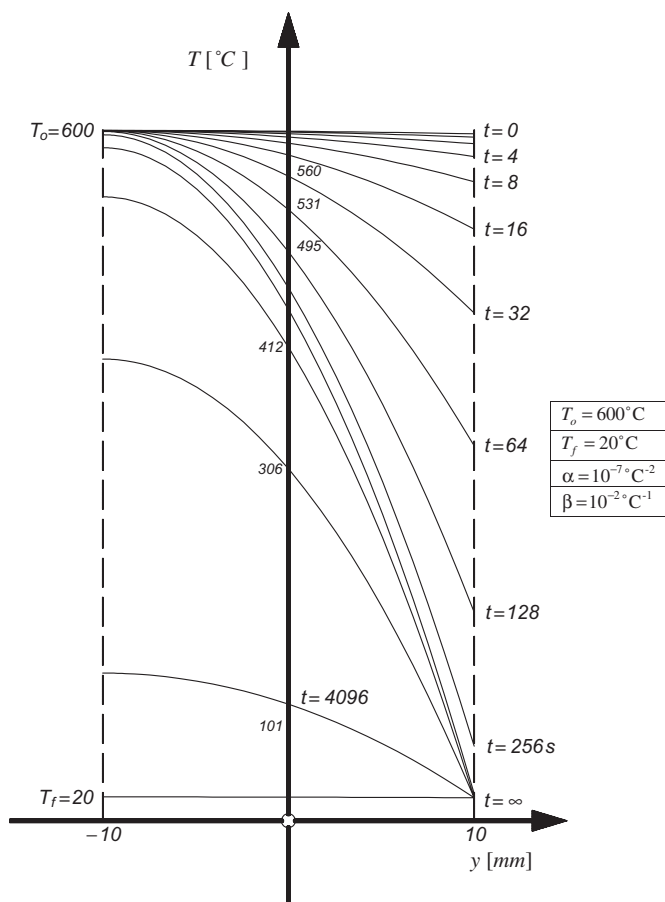


Fig. 9. Heat curving thermal history (1st case).

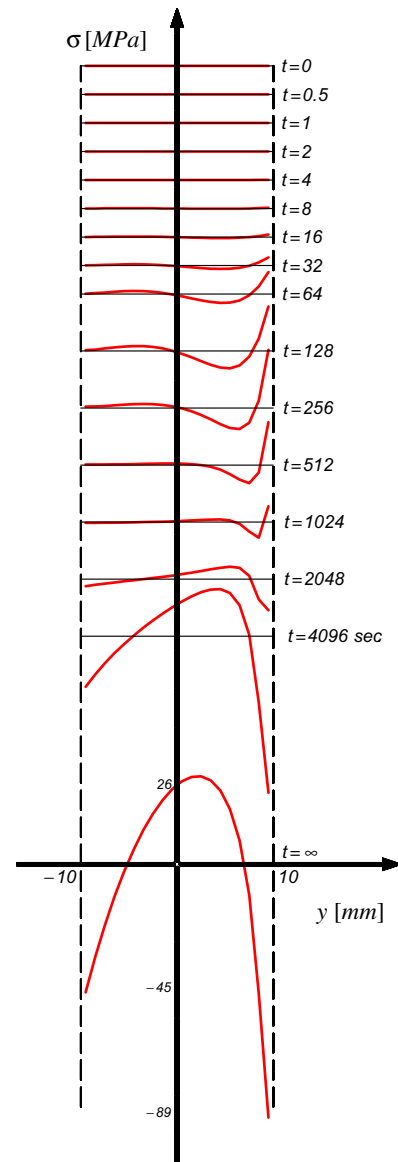


Fig. 11. Heat curving eigen-stresses generation (1st case).

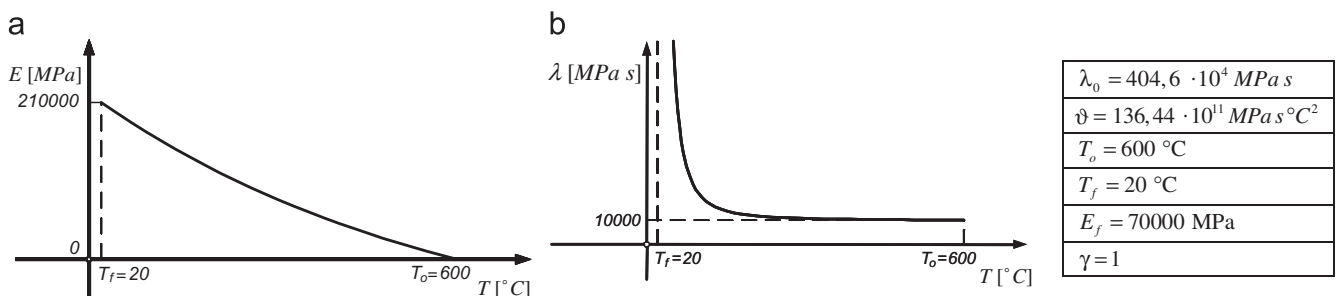


Fig. 10. (a) Elastic modulus versus temperature. (b) Viscous coefficient versus temperature.

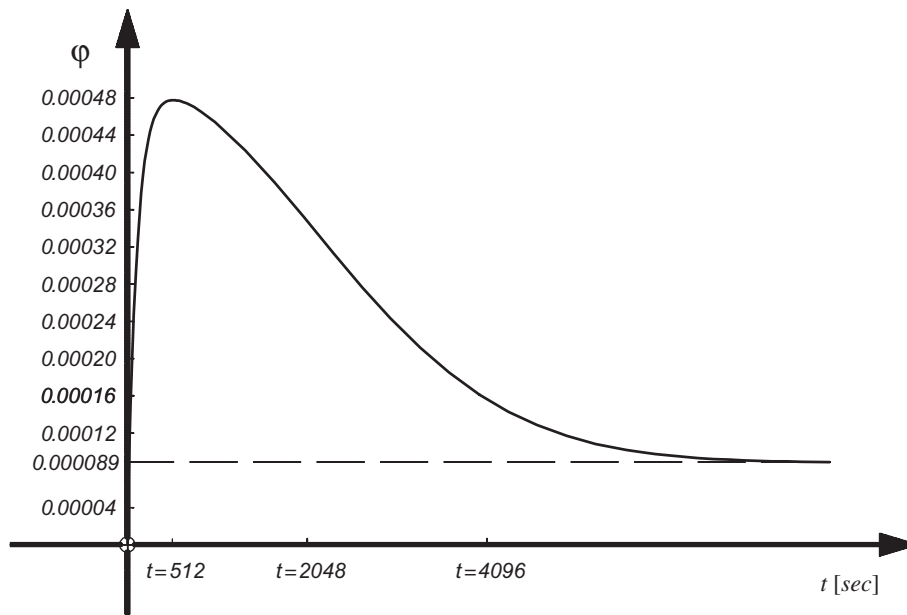


Fig. 12. Normalized curvature generation (1st case).

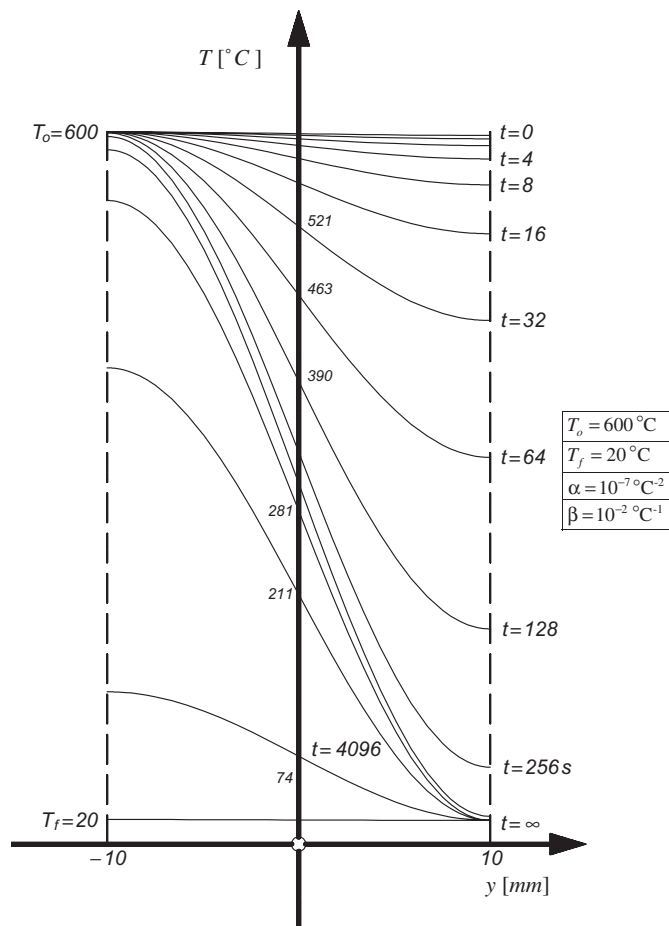


Fig. 13. Heat curving thermal history (2nd case).

In this case the temperature of the outer surfaces diminishes in the first 4 s of about 500 °C. Conspicuous gradients are thus suddenly formed and persist practically

unchanged for almost 250 s. The process completely ends after circa 4000 s.

The temperature dependence of the elastic modulus and of the viscosity coefficient is assumed to be here the same of the preceding example (see Figs. 5a and b).

Fig. 8 shows some isochronous curves of the tempering eigen-stresses.

The sign inversion occurs in this case later compared with the previous example ( $t = 2048$  s) but thanks to the increased value of the thermal gradients, surface compressions reach now the intensity of about 86 MPa and middle tensions reach 51 MPa.

#### 4.2. Asymmetrical cooling

##### 4.2.1. Heat curving: first case

Let us suppose that a  $2\delta$  thick steel sheet undergoes the following thermal history (see Fig. 9)

$$T(y, t) = \frac{T_A(t) - T_B(t)}{2} \left[ -2 \left( \frac{y}{2\delta} \right)^2 - 2 \left( \frac{y}{2\delta} \right) + \frac{1}{2} \right] + \frac{T_A(t) + T_B(t)}{2}, \quad (4.6)$$

where

$$T_A(t) = T_f + (T_0 - T_f) e^{-\alpha t^2} \quad (4.7a)$$

and

$$T_B(t) = T_f + (T_0 - T_f) e^{-\beta t}, \quad (4.7b)$$

with  $\alpha = 10^{-7} \text{ } ^\circ\text{C}^{-2}$ ,  $\beta = 10^{-2} \text{ } ^\circ\text{C}^{-1}$  and the initial and final temperature are, respectively, equal to  $T_0 = 600 \text{ } ^\circ\text{C}$  and  $T_f = 20 \text{ } ^\circ\text{C}$ .

The temperature dependence of the elastic modulus and the viscosity coefficient is given, following Sen et al. [2], by

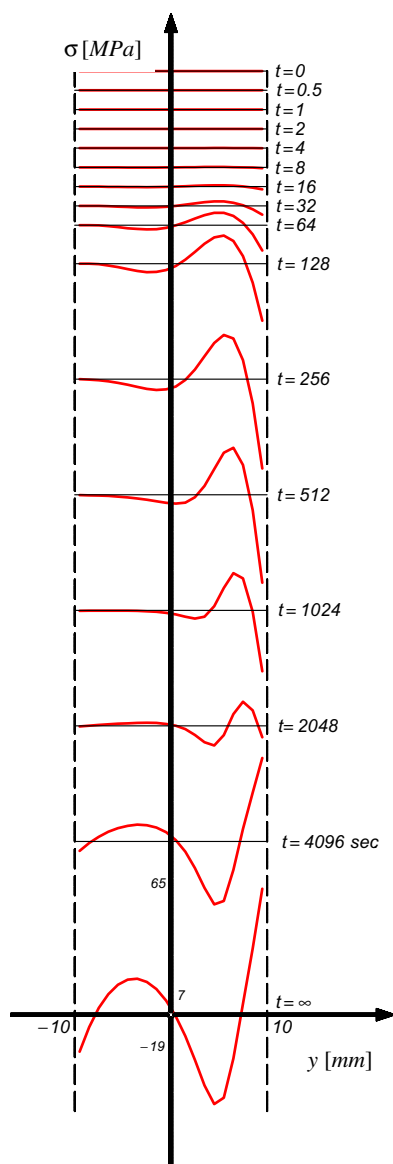


Fig. 14. Heat curving eigen-stresses generation (2nd case).

(4.5a) and (4.5b), where we posed  $E_0 = 0$  MPa and  $E_f = 210\,000$  MPa (see Figs. 10a and b).

Figs. 11 and 12, respectively, illustrate the time generation of eigen-stresses and of the curvature, normalized in  $2\delta$ .

It can be observed that, due to the asymmetry of the process, final eigen-stresses are also asymmetric and compression stresses are more intense at the face which was first submitted to a rapid cooling.

The time progression of the normalized curvature can be divided into two periods: during the first part it increases very steeply with a maximum at circa 525 s. In the second period the curvature  $\varphi$  diminishes but approaches asymptotically the final permanent value of about  $8.9 \times 10^{-5}$ .

#### 4.2.2. Heat curving: second case

We suppose now to submit the same steel sheet to a different shaped thermal history, described by Eq. (4.8) and

illustrated in Fig. 13.

$$T(y, t) = \frac{T_A(t) - T_B(t)}{2} \cos\left(\pi \frac{y + \delta}{2\delta}\right) + \frac{T_A(t) + T_B(t)}{2}, \quad (4.8)$$

where  $T_A(t)$ ,  $T_B(t)$ ,  $E(T)$ ,  $\lambda(T)$  are the same of the preceding example. Figs. 14 and 15, illustrate, respectively, the time generation of eigen-stresses and of the curvature, normalized in  $2\delta$ .

It can be noticed that eigen-stresses do not assume in this case the typical form of an inverted U but rather that of a sort of sinusoidal curve.

The overall time progression of the normalized curvature well resemble that of the preceding example with the only difference that now, during the second period, the diminishing branch overcomes zero, that is, the curvature  $\varphi$  surprisingly changes sign and the residual final value asymptotically approaches a negative value ( $-4.3 \times 10^{-5}$ ).

In other words, the final bending effect strongly depends on the type of thermal history and it can even develop in the opposite way to the desired one since, as in the present case, the plate can even protrude, at the end, towards the face that was cooled first.

## 5. Conclusions

During thermal treatments like glass tempering, steel toughening or heat curving, plane plates achieve their final state of solid consistence through different cooling processes, instantly non-uniform over the thickness being submitted at the same time to complex, transient and heterogeneous evolutions of their visco-elastic properties.

Consequently, eigen-stresses and deformations continuously change with time during this transition phase and tend to final values whose knowledge is of great practical importance but rather difficult to be foreseen.

In this paper this prediction is analytically pursued by means of a very simple discrete rheological model composed by a parallel assemblage of Maxwell chains made of elements whose mechanical properties are temperature dependant.

The stiffening process is simulated by attributing to each element known temperature-dependant visco-elastic properties, which tend to the final values of the solid phase within the transition interval, and by assuming known temperature histories of regular although whatever form.

The model demonstrates ability to qualitatively well reproduce, in a very straightforward and explicit way, the time development of eigen-stresses and residual deformations all along thermal treatments of whatever kind and appears therefore well suited, after the necessary calibrations, for theoretical predictions about thermo-mechanical effects following treatments like tempering in glass plates and heat curving in steel beams.

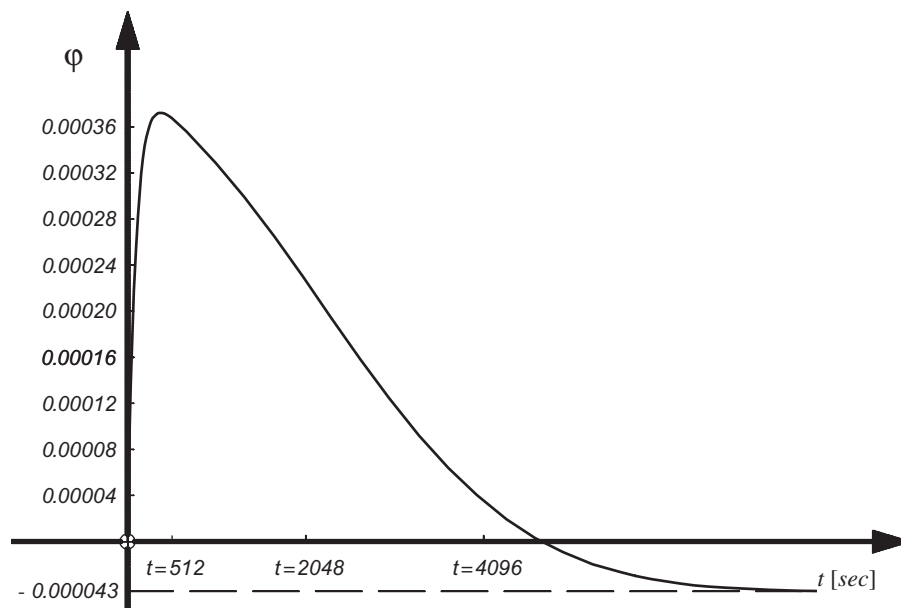


Fig. 15. Normalized curvature generation (2nd case).

### Acknowledgement

The present study has been carried on with the financial support of the Italian Ministry of University and Research (MIUR).

### References

- [1] Froli M, Masiello G. Campi termici instazionari nella fase di idratazione di getti massicci in calcestruzzo interagenti con l'ambiente. *L'Industria Italiana del Cemento* 2004;797:332–46.
- [2] Sen R, Gergess AN, Issa C. Finite-element modeling of heat-curved I-girders. *Journ. of Bridge Engineering* 2003; 153–161.
- [3] Cristescu N, Suliciu I. *Viscoplasticity*. The Hague: Martinus Nijhoff; 1982.
- [4] Drozdov AD. *Mechanics of viscoelastic solids*. New York: Wiley; 1998.
- [5] Kanninen MF, Adler WF, Rosenfield AR, Jaffee RI. (editors). *Inelastic behavior of solids*. Ohio: Battelle Institute Materials Science Colloquia, Columbus and Atwood Lake; 1969.
- [6] Achenbach M, Müller I. Creep and yield in martensitic transformations. *Ingenieur Archiv* 1983;73–83.
- [7] Müller I, Sahota HS, Villaggio P. On the thermodynamics of repetitive visco-plastic moulding. *Zeitschrift Für Angewandte Mathematik and Physik* 2002;1140–9.
- [8] Bažant ZP. Constitutive equation for concrete creep and shrinkage based on thermodynamics of multiphase systems. *Matériaux et Constructions* 1970;13:3–36.
- [9] Carol I, Bažant ZP. Viscoelasticity with aging caused by solidification of nonaging constituents. *Journal of Engineering Mechanics, ASCE* 1993;119:2252–68.
- [10] Nagy A. Simulation of thermal stress in reinforced concrete at early ages with a simplified model. *Matériaux et Constructions* 1997;30:167–73.
- [11] Lee EH, Rogers TG, Woo TC. Residual stresses in a glass plate cooled symmetrically from both surfaces. *Journal of the American Ceramic Society* 1963;48:36–128.
- [12] Narayanaswamy OS, Gardon R. Calculation of residual stresses in glass. *Journal of the American Ceramic Society* 1969;52:554–8.
- [13] Gardon R, Narayanaswamy OS. Stress and volume relaxation in annealing flat glass. *Journal of the American Ceramic Society* 1970;53:380–5.
- [14] Narayanaswamy OS. A model of structural relaxation in glass. *Journal of the American Ceramic Society* 1971;54:491–8.
- [15] Narayanaswamy OS. Stress and structural relaxation in tempering glass. *Journal of the American Ceramic Society* 1978;61:146–52.
- [16] Kurkjian CR. Relaxation of torsional stress in the transformation range of a soda-lime-silica glass. *Physics and Chemistry of Glasses* 1963;4:36–128.
- [17] Soules TH, Rekhson SM, Markovsky A. Finite element calculation of stresses in glass parts undergoing viscous relaxation. *Journal of the American Ceramic Society* 1987;70:90–5.
- [18] Laufs W. Ein Bemessungskonzept zur Festigkeit thermisch vorgespannter Gläser, vol. 45. *Schriftenreihe Stahlbau-RWTH Aachen*; Heft: 2000 p. 28–41 [Section 2.2.3].
- [19] Gardon R. Calculation of temperature distributions in glass plates undergoing heat-treatment. *Journal of the American Ceramic Society* 1958;41:200–9.
- [20] Wolfram S. *The mathematica book*, 5th ed. Wolfram Media; 2003.